Selective desorption of organophosphonates on chemically functionalized titanium by Direct Laser Patterning

M.A. Fernández-Rodríguez, M.A. Rodríguez-Valverde, M.A. Cabrerizo-Vílchez

Biocolloid and Fluid Physics Group, Applied Physics Department, Faculty of Sciences, University of Granada, 18071 Granada (Spain)

Abstract

Surface functionalization based on organophosphonate molecules and Direct Laser Patterning (DLP) technique both allow to design chemically patterned titanium surfaces devoted to biomaterial engineering. Ultrapolished surfaces of commercially pure titanium were modified with 16-phosphonohexadecanoic acid and octadecylphosphonic acid. The DLP technique with a green pulsed laser was applied to selectively desorb the organophosphonate molecules on the functionalized titanium surfaces. Three regimes of laser ablation were found on the bare titanium surfaces as the ratio between the spot diameter and the interspot distance. Finally, the organophosphonate functionalized titanium surfaces subjected to DLP revealed different wettability domains with minimum impact on the roughness, validated by XPS, AFM and ESEM.

Keywords: Titanium, Chemical functionalization, Organophosphonate, Laser patterning, Biomaterial engineering

1. Introduction

A well-established strategy to change the surface properties of titanium is the chemical functionalization with organophosphonates [1, 2, 3]. These molecules are composed of a phosphonate head ($-PO_3^{-2}$), which is able to

Email address: marodri@ugr.es (M.A. Rodríguez-Valverde)

anchor to the titanium dioxide (TiO_2) [2], a hydrocarbon chain and a terminal group. The terminal group will determine the final surface properties of the functionalized surface. This functionalization does not change the surface roughness of titanium at a micrometric scale. Anchoring of organophosphonates to the titanium surface is mechanically resistant, chemically stable and it enables the interaction with biomolecules [4].

Direct Laser Patterning (DLP) technique allows to produce wettability templates on chemically modified surfaces [5]. The DLP technique enables the localized desorption of molecules on the surface through direct laser ablation. The selective ablation produces different wettability domains on the surface where bare zones coexist with zones covered with the corresponding molecule. These patterns may be useful for directed cell growth [6, 7].

The current study aims to establish a minimally invasive protocol for the wettability patterning of ultrapolished commercially pure titanium surfaces using the DLP technique. Smooth titanium surfaces were functionalized with two organophosphonate molecules with different terminal groups (methyl and carboxyl groups, respectively). A commercial DLP device was applied on the chemically-modified titanium surfaces.

2. Materials and Methods

2.1. Sample preparation

Commercially pure ASTM grade II [8] titanium ingots (Manfredi) were cut into discs (1.6 cm diameter, 1.6 mm thickness). Next, the samples were ultrapolished with a grinder/polishing machine (Beta Grinder Polisher, Buehler). The samples reached very low values of roughness after polishing (< 1 nm, measured with an atomic force microscope over an area of $1\,\mu\text{m}^2$).

After ultrapolishing, residual glue and polishing agents were found on the titanium samples. The samples were cleaned in ultrasonic baths of acetone, soapy water, ethanol and distilled water and finally, MilliQ water. Next, the samples were dried with N_2 gas. The samples were stored at this point in Petri dishes to prevent eventual pollution. The stored samples were cleaned by immersion in an acetone ultrasonic bath and further by drying with N_2 gas. Once the samples were "refreshed" with the acetone bath, they were prepared to obtain a good coverage of organophosphonate. It is known that the best conditions for the molecule bonding are achieved with the maximum amount of TiO_2 on the titanium surface [2]. Also, it is necessary to minimize any pollutant and water on the titanium surface [2, 9]. In order to satisfy

these conditions, a radio frequency plasma device (KX1050 Plasma Asher, Emitech) with argon gas was used to remove the hydrocarbon pollutants on the titanium surface. The plasma treatment was performed for 15 min. at a power of 25 W and a gas flow rate of 15 ml/min. Next, the samples were immersed in MilliQ water overnight to reach a controlled oxidation state. Finally, the titanium samples were heated in an oven at 180 °C for 30 min. to dehydrate the titanium surface. The samples were isolated during heating in a clean sealed glass dish and finally, they were stored before and after each treatment in Petri dishes to prevent pollution.

Two solutions of 16-phosphonohexadecanoic acid (16-HXA, Sigma Aldrich) and octadecylphosphonic acid (ODPA, Sigma Aldrich) at 1 mM in tetrahydrofuran (THF, Sigma Aldrich) were prepared to functionalize the titanium surfaces. Both molecules have similar hydrocarbon chain length but different terminal groups: an apolar methyl group $-CH_3$ in ODPA and a polar carboxyl group $-COOH$ in 16-HXA. The clean and dry samples were immersed in the organophosphonate solution during five days in dark. In order to stabilize the organophosphonate functionalized surfaces, we applied the protocol reported by Hanson et al. [10] to stabilize the organophosphonate molecules on the titanium surface. Thereby, the samples were dried with N_2 and argon gas and next, they were heated at 140 °C for 1 h. Next, the organophosphonate excess was removed in a ultrasonic bath of K_2CO_3 (Sigma Aldrich) at 0.5 M (2:1 ethanol:water) for 1 min., and next 5 min. in a ultrasonic bath of MilliQ water. Finally the samples were dried with N_2 gas.

A commercial set up of DLP (Laser E-20 SHG II, Rofin) was used. This device has a Nd:YAG green pulsed laser with 512 nm of wavelength. Two motorized mirrors redirect the beam laser to the desired point through a 100 mm focal lens that focuses the laser beam in the maximum ablation point. The relevant input parameters of the laser system are the laser beam intensity or laser fluence, I, the laser beam speed, v, and the pulse repetition rate, ν. The output parameters that describes the laser ablation are the interspot distance, D, and the diameter of spots, d. The main goal was to reach the minimum ablation on the titanium surfaces measurable with White Light Confocal Microscopy (see next Section). The surfaces were analyzed just after each laser treatment to avoid significant aging of the samples.

2.2. Surface chemistry and topography

The surface chemistry of the titanium surfaces was quantified from X-ray Photoelectron Spectroscopy (XPS, Axis Ultra-DLD, Kratos). The maximum

depth resolution of the XPS device was lower than 10 nm.

The ablation profiles of the titanium surfaces were acquired with a White Light Confocal Microscope (WLCM, PLμ Confocal Imaging Profiler, Sensofar). WLCM provided topography images with a height resolution of 0.1 μm at 150x magnifications. These topography images enabled to measure the laser spot diameter and the interspot distance by fitting circles or lines to the ablated regions. Environmental Scanning Electronic Microscope (ESEM, Quanta 400, FEI) was used to obtain high resolution backscattered electron images and to visualize the chemical patterning of the titanium surfaces. Height and phase images were also acquired with an Atomic Force Microscope (AFM, MultiMode Scanning Probe Microscope Nanoscope IV, Veeco) in tapping mode over $50 \times 50\,\mu\mathrm{m}^2$ regions. The phase images provide the best contrast of fine morphological and nanostructural features. The arithmetic average of height deviations respect to the central plane (R_a) and the standard deviation of heights (R_q) were estimated from the AFM height images.

3. Results and Discussion

3.1. Surface cleaning

The surface chemical composition of the titanium surfaces were studied by XPS analysis to monitor the cleaning treatment. The surface atomic percentages of the main chemical species, $Ti\,2p$, $O\,1s$ and $C\,1s$ (pollutants), are listed in Table 1. Also, the $O\,1s$ spectra were deconvoluted into two peaks, one at ~ 530.4 eV corresponding to TiO_2 and another at ≥ 531 eV corresponding to water, hydroxyl groups or non stoichiometric oxides TiO_x [11]. The surface atomic percentages of $O\,1s$ corresponding to TiO_2 are also listed in Table 1.

It can be observed in Table 1 that the titanium surfaces were polluted with the "refreshing" acetone ultrasonic bath. Otherwise, the argon plasma treatment caused the lowest surface pollution ($C\,1s$) and the highest $Ti\,2p$ and $O\,1s$ percentages. This suggests that the titanium oxides emerged over the pollutants. The plasma-treated samples revealed the maximum percentage of $O\,1s$ corresponding to TiO_2 although the later water immersion produced a decrease of the TiO_2 signal. The argon plasma treatment exhibited a remarkable aging effect due to the active surface sites generated [12] but the MilliQ water immersion stabilized the oxidation state of the titanium surfaces. Finally, the dry heating slightly increased the TiO_2 amount while it provided a water-free titanium surface.

Table 1: Surface atomic percentages of the main chemical species found in the titanium surfaces prior to the functionalization with organophosphonate molecules.

	Surface atomic percentage for each treatment (%)				
	Ultrasonic baths	Acetone "refreshing"	Argon plasma	Water oxidation	Dry heating
$Ti\,2p$	20.0	18.8	26.4	25.3	25.2
$O\,1s$	54.2	50.2	63.8	61.9	60.6
$C\,1s$	25.8	31.7	9.8	12.8	14.2
$O\,1s$ surface atomic percentage in the form of TiO_2 for each treatment (%)					
	63	60	76	69	71

Table 2: Surface atomic percentages of the main chemical species found in the titanium surfaces modified with organophosphonate molecules.

	Surface atomic percentage (%)		
	No molecule (only THF)	ODPA	16-HXA
$Ti\,2p$	24.9	21.8	18.8
$O\,1s$	58.8	54.5	52.8
$C\,1s$	16.3	22.7	26.8
$P\,2p$	0.0	1.1	1.7

3.2. Surface functionalization with organophosphonates

XPS analysis were performed on 16-HXA and ODPA functionalized titanium surfaces, following the protocol described in Section 2.1. The XPS results summarized in Table 2 revealed no functionalization (no presence of phosphorus $P\,2p$) when only THF was used, as expected. The surfaces functionalized with 16-HXA and ODPA revealed similar phosphorus signals and lower $Ti\,2p$ and $O\,1s$ signals respect to the THF immersion. This points out to a coverage of the titanium surfaces with the corresponding organophosphonate molecule.

3.3. Tunning-up of laser ablation

For the adjustment of the DLP technique, the clean ultrapolished titanium surfaces described in Section 3.1 were ablated with different laser parameters. Once the speed v and the intensity I were fixed, an increase in frequency ν reduced the ablation over the sample. In order to produce

observable ablation, the minimum frequency (15 kHz) was used. Under these conditions, the minimum diameter of a single spot produced on the titanium surface was $d_{min} = 10\,\mu$m.

The interspot distance was systematically varied by changing the speed of laser beam in the range between 10 mm/s and 300 mm/s. The results revealed three ablation regimes as the interspot distance increased. Continuous line (Fig. 1a), overlapping spots (Fig. 1b) and non-overlapping spots (Fig. 1c). All spots presented "crater" shape with a deep center rounded by high edges produced by the reflux of molten titanium [13, 14]. The spot diameter in terms of the interspot distance and the corresponding beam speed are plotted in Fig. 2. This graph enables to select the intensity and the beam speed, at the fixed frequency of 15 kHz, for obtaining an ablation regime on the titanium surfaces, i.e. a desired ratio between spot diameter d and interspot distance D. For a fixed intensity, the interspot distance increased with the speed of the laser beam, as expected. However, there was a slight increase of the spot diameter with the speed of the laser beam. This behavior can be explained in terms of the reflux of molten titanium as the laser ablated several times a given point for the overlapping spots and continuous lines. This repeated ablation might cause the refilling of the "crater-like" spot with the molten titanium, decreasing the spot diameter. The interspot distance remained constant for different laser beam intensities although the spot diameter increased with the laser intensity, as expected.

3.4. Wettability patterning of smooth titanium surfaces

When the laser beam was focused at a desired point on each titanium surface, the molten material reflux always increased the surface roughness. Thereby, we intended to reach a balance between energetic laser ablation and minimum alteration of roughness. Using the results from Section 3.3, the following input parameters were fixed:

- Laser pulse frequency $\nu = 15$ kHz.
- Laser beam speed $v = 50$ mm/s.
- Intensities varying between 11.0 A and 11.5 A.

Under these conditions of laser ablation, we expected to be in the ablation regime $d = D$, i.e. touching spots. This regime avoids to ablate more than once each region of the surface. In Table 3 are presented the measured spot

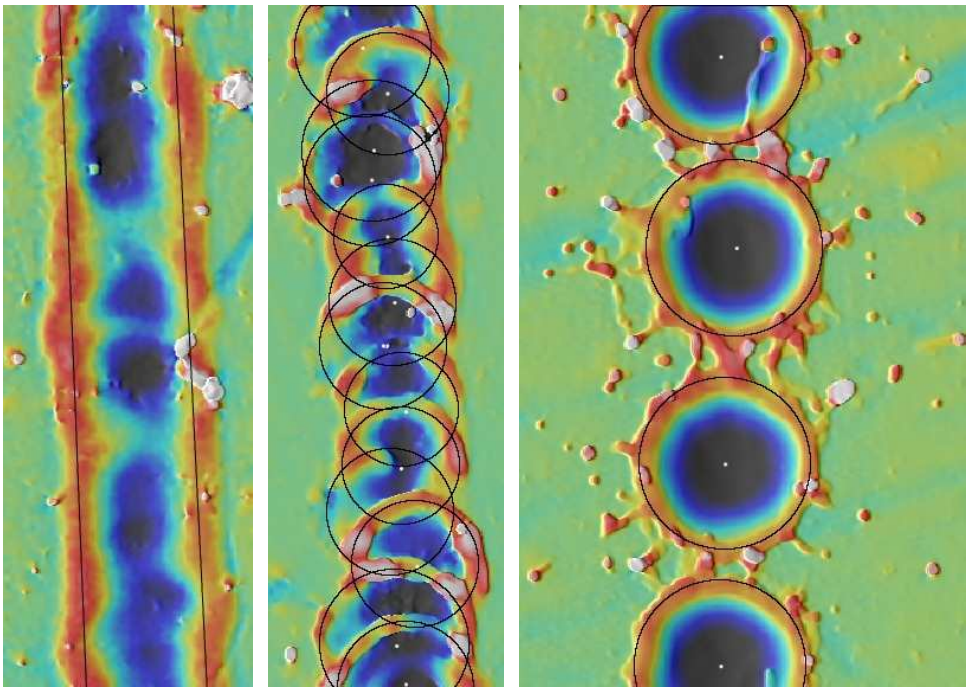

(a) (b) (c)

Figure 1: Regimes of DLP on smooth titanium surfaces illustrated with WLCM images: (a) continuous line for $I = 12.5$ A, $v = 10$ mm/s and $\nu = 15$ kHz ($23 \times 64\,\mu\text{m}^2$ image), (b) overlapping spots for $I = 12.5$ A, $v = 75$ mm/s and $\nu = 15$ kHz ($22 \times 64\,\mu\text{m}^2$ image) and (c) non-overlapping spots for $I = 12.3$ A, $v = 290$ mm/s and $\nu = 15$ kHz ($41 \times 64\,\mu\text{m}^2$ image).

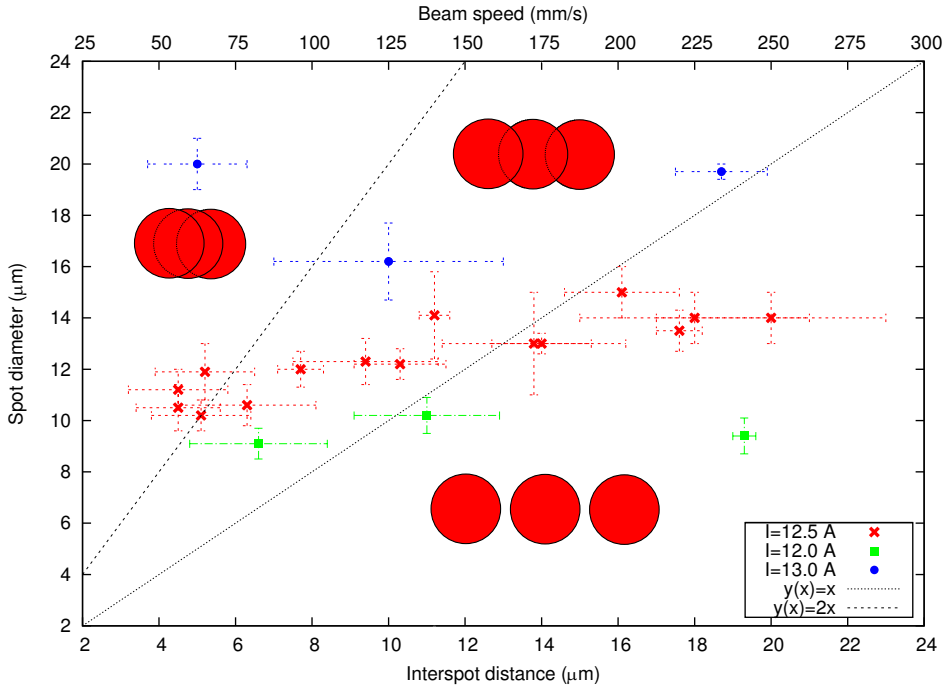

Figure 2: Spot diameter in terms of the interspot distance for ultrapolished titanium surfaces subjected to DLP at fixed frequency of 15 kHz. In the upper-axis, the corresponding beam speed is also plotted. The two discontinuous lines in the plot separates the three regimes of laser ablation.

Table 3: Spot diameter d and interspot distance D for the titanium surfaces functionalized with ODPA and 16-HXA molecules and subjected to DLP with $\nu = 15$ kHz, $v = 50$ mm/s and different intensities I. The dimensions were measured over the WLCM topography images. The roughness parameters of the regions subjected to laser ablation and the non-ablated regions were measured with AFM over a scansize of $424\,\mu\text{m}^2$.

	I (A)	d (nm)	D (nm)	R_a, R_q (nm) ablated region	R_a, R_q (nm) non-ablated region
ODPA	11.5	5.2±0.5	5.3±0.7	39.4, 51.4	11.7, 17.6
16-HXA	11.2	6.0±0.6	8±3	14.8, 18.4	9.4, 16.1

diameter, interspot distance and the roughness parameters R_a and R_q of the ablated and non-ablated regions of the functionalized titanium surfaces described in Section 3.2. The spot diameter agreed with the interspot distance. As expected, it was found more roughness in the ablated regions than in the non-ablated regions although the values were always below micrometer scale.

In the AFM height images of Fig. 3 the ablated regions (rougher) are clearly distinguished. The phase images also reveal fine differences between the regions subjected to laser ablation and the non-ablated regions. The greater ablation at the pattern border allowed to easily distinguish both two regions.

Annular laser ablations were performed on the ODPA and 16-HXA functionalized titanium surfaces. The backscattered electron ESEM images in Fig. 4 revealed differences between the ablated regions and the non-ablated regions for both organophosphonate molecules. The bare regions of the titanium surfaces were brighter and homogeneous. Instead, the regions covered by the organophosphonate molecule were darker and heterogeneous. The XPS analysis in Table 4 confirmed that the $P\,2p$ (from the organophosphonate head) and the $C\,1s$ (from the hydrocarbon chain of the organophosphonate) signals decreased for both ODPA and 16-HXA functionalized titanium surfaces on the region subjected to DLP. This confirmed that the laser beam partially desorbed the organophosphonates. In the case of the 16-HXA functionalized titanium surfaces, the ablated region revealed a null signal of phosphorus, so that the laser completely removed the organophosphonate coverage. In this case, the remaining $C\,1s$ signal was due to adventitious

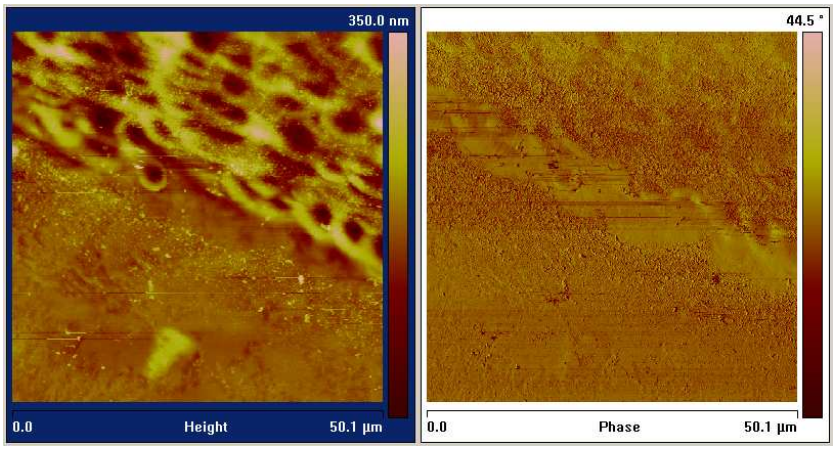

(a)

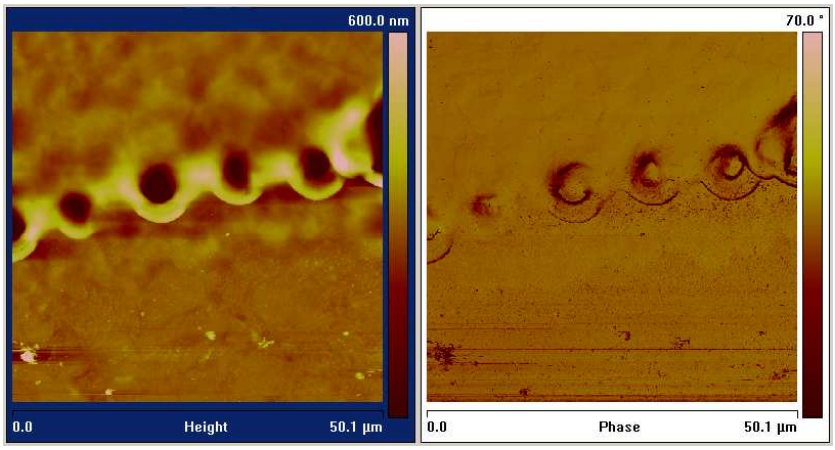

(b)

Figure 3: AFM height and phase images of the patterned titanium surfaces ($50 \times 50\,\mu m^2$): (a) ODPA and (b) 16-HXA organophosphonates. The laser ablation at the pattern border region was deliberately marked with deeper spots.

Table 4: Surface atomic percentages of the main chemical species in the ODPA and 16-HXA functionalized titanium surfaces, subjected to DLP.

	Surface atomic percentage (%)			
	ODPA		16-HXA	
	DLP region	No DLP region	DLP region	No DLP region
$Ti2p$	24.0	21.8	28.5	18.8
$O1s$	58.3	54.5	56.8	52.8
$C1s$	17.1	22.7	14.7	26.8
$P2p$	0.6	1.1	0.0	1.7

pollutants on the surface. On the ablated regions, the $Ti\,2p$ and $O\,1s$ signals associated to TiO_2 increased.

For illustrative purposes, several MilliQ water drops were deposited on the rings produced with DLP (bare regions). The top-view images (Fig. 5) show the wettability contrast between surface regions subjected and non-subjected to DLP. The wettability contrast was greater for the ODPA surface than for the 16-HXA surface. It is known that the contact angle of well-prepared smooth surfaces of titanium is greater than the contact angle of carboxyl-modified surfaces [3]. Although the laser treatment of titanium may decrease the contact angle [13], the resulting wettability contrast will be negative or even zero: the confinement of liquid in the bare region is not favoured. In other respects, the XPS results of Table 4 show that the ODPA surface concentration dropped by half in the DLP subjected regions, instead of the fully removal of organophosphonate produced in the 16-HXA surface. However, the significant hydrophobicity of the methyl terminal group [2] explains the positive wettability contrast found in the patterned ODPA surface: the liquid is constrained at the border.

4. Conclusions

The Direct Laser Patterning technique was tuned up and successfully applied to smooth titanium surfaces modified separately with two organophosphonate molecules: octadecylphosphonic acid ($-CH_3$ terminal group) and 16-phosphonohexadecanoic acid ($-COOH$ terminal group). The desorption of the organophosphonate molecules was validated by XPS analysis. The surface roughness, after DLP, was remained below the micrometer scale. The

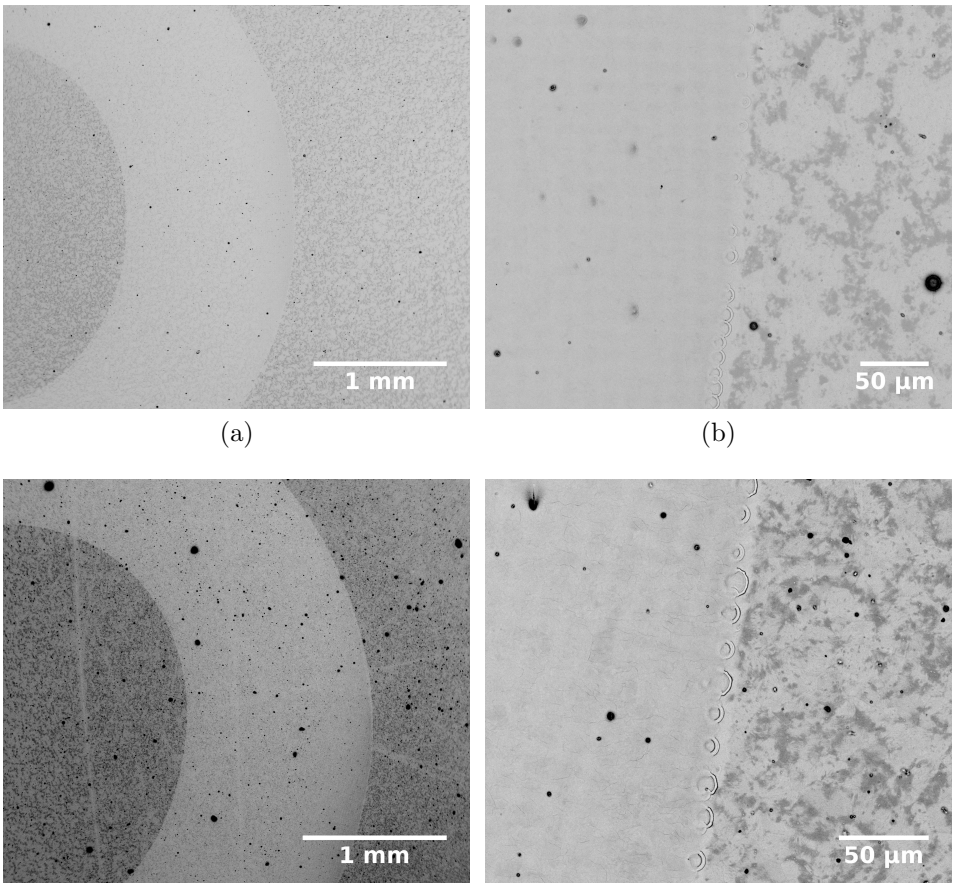

Figure 4: Backscattered electron ESEM images. (a) ODPA functionalized titanium surface subjected to annular laser ablation, (b) a magnified image of the surface in (a), (c) 16-HXA functionalized titanium surface subjected to annular laser ablation and (d) a magnified image of the surface in (c). The laser ablation at the pattern border region was deliberately marked with depper spots.

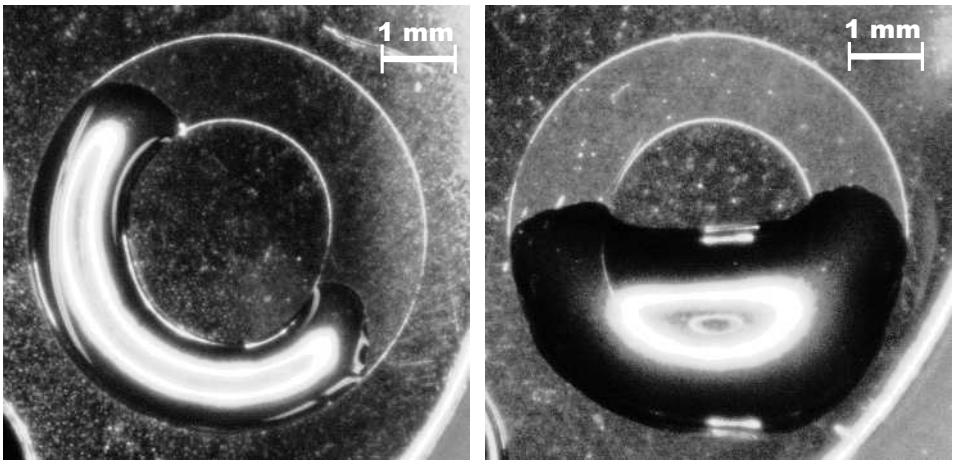

(a) (b)

Figure 5: Top-view images of titanium surfaces functionalized with (a) ODPA and (b) 16-HXA molecules and subjected to annular laser ablation. Several MilliQ water drops were deposited over each surface to illustrate the final wettability contrast.

surface differences between ablated and non-ablated regions were revealed by AFM, ESEM and wettability tests. The minimum size of feature produced with the DLP technique on ultrapolished titanium was 10 μm. Three regimes of ablation were found as the ratio between the spot diameter and the interspot distance: continuous lines, overlapping spots and non-overlapping spots. The selective desorption of organophosphonate molecules on functionalized titanium surfaces might be used to design wettability patterns with submicrometer roughness, which might be helpful for directed cell growth in implantology.

Acknowledgements

This study was supported by the "Ministry of Science and Innovation" (project MAT2011-23339) and by the "Junta de Andalucía" (projects P08-FQM-4325, P09-FQM-4698 and P10-FQM-5977). Authors thank to J.A. Martín-Perez, who masterly polished the titanium samples, and Y. Sanchez-Treviño, C.L. Moraila-Martínez and Dr. F.J. Montes Ruiz-Cabello for fruitful discussions.

References

[1] E. S. Gawalt, M. J. Avaltroni, N. Koch, J. Schwartz, Self-assembly and bonding of alkanephosphonic acids on the native oxide surface of titanium, Langmuir 17 (19) (2001) 5736–5738.

[2] S. Tosatti, Functionalized titanium surfaces for biomedical applications: physico-chemical characterization and biological in vitro evaluation. diss. eth no. 15095, Ph.D. thesis, Swiss Federal Institute of Technology Zurich (2003).

[3] J. Wu, I. Hirata, X. Zhao, B. Gao, M. Okazaki, K. Kato, Influence of alkyl chain length on calcium phosphate deposition onto titanium surfaces modified with alkylphosphonic acid monolayers, J. Biomed. Mater. Res. A (2013) In pressdoi:10.1002/jbm.a.34545.

[4] M. P. Danahy, M. J. Avaltroni, K. S. Midwood, J. E. Schwarzbauer, J. Schwartz, Self-assembled monolayers of α, ω-diphosphonic acids on Ti enable complete or spatially controlled surface derivatization, Langmuir 20 (13) (2004) 5333–5337.

[5] M. Shadnam, S. Kirkwood, R. Fedosejevs, A. Amirfazli, Direct patterning of self-assembled monolayers on gold using a laser beam, Langmuir 20 (7) (2004) 2667–2676.

[6] H. Craighead, C. James, A. Turner, Chemical and topographical patterning for directed cell attachment, Curr. Opin. Solid St. M. 5 (2-3) (2001) 177–184.

[7] M. Morra, Biomolecular modification of implant surfaces, Expert. Rev. Med. Devices 4 (3) (2007) 361–372.

[8] G. Welsch, R. Boyer, E. Collings, Materials properties handbook: titanium alloys, Materials properties handbook, ASM International, 1994.

[9] H. Butt, K. Graf, M. Kappl, Physics and chemistry of interfaces, Wiley-VCH, 2003.

[10] E. Hanson, J. Schwartz, B. Nickel, N. Koch, M. Danisman, Bonding self-assembled, compact organophosphonate monolayers to the native oxide surface of silicon, J. Am. Chem. Soc. 125 (51) (2003) 16074–16080.

[11] C. Wagner, W. Riggs, L. Davis, J. Moulder, Handbook of X-ray Photoelectron Spectroscopy, 1st Edition, Perkin-Elmer Corporation (Physical Electronics), 1979.

[12] W. Birch, A. Carré, K. Mittal, Wettability techniques to monitor the cleanliness of surfaces, in: R. Kohli, K. Mittal (Eds.), Developments in Surface Contamination and Cleaning, William Andrew, Inc, 2008, pp. 1–32.

[13] J. Lawrence, L. Hao, H. Chew, On the correlation between Nd : YAG laser-induced wettability characteristics modification and osteoblast cell bioactivity on a titanium alloy, Surf. Coat. Tech. 200 (18-19) (2006) 5581–5589.

[14] J. Conde, P. González, F. Lusquios, S. Chiussi, J. Serra, B. León, Analysis of plume deflection in the silicon laser ablation process, Appl. Phys. A-Mater. 88 (2007) 667–671.